Elucidating Jet Energy Loss in Heavy Ion Collisions

Nathan Grau Columbia University, Nevis Laboratories
representing the ATLAS Collaboration

Jet Reconstruction

Cone jet reconstruction requires a determination and subtraction of the average background E_T. This subtraction is E_T-, η-, and layer-dependent. The calorimetric tower (ΔηxΔφ = 0.1x0.1) E_T distribution before/after subtraction is shown in the upper/lower panel of Fig. 1. A standard seeded cone algorithm is then run with R=0.4 and a seed tower of 5 GeV where R = $\sqrt{\Delta\phi^2 + \Delta\eta^2}$.

For k_T jet reconstruction the *FastJet* implementation of Cacciari and Salam is used with D=0.4, the parameter which defines the extent of the clustering. This results in jet reconstruction performed directly on the heavy ion event without background subtraction. Each tower in the event is incorporated into a jet (see lower left panel of Fig. 2). Since most reconstructed jets are primarily composed of background energy, discrimination variables are used to separate true jets from the background jets. The maximum-to-average tower E_T in a jet is one example. The background jets are then used to determine the background energy to subtract from the true jets.

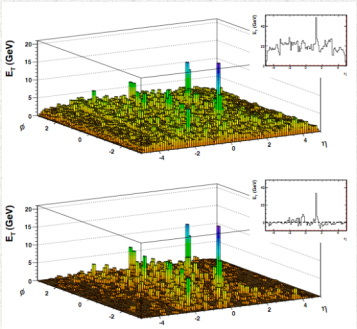

Fig. 1 Example of background subtraction for cone jet reconstruction. *Upper:* tower energies from PYTHIA embedded di-jets visible above the HIJING background. *Lower:* tower energies after subtraction. Inset shows the projection in η of towers from -0.5 < φ < -1.5.

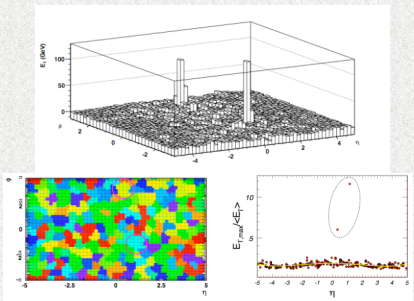

Fig. 2 Example of fast k_T jet reconstruction. *Upper:* tower energies with PYTHIA embedded di-jet visible above the HIJING background. *Lower left:* colored region corresponds to a reconstructed jet. *Lower right:* Maximum-to-average tower energy for each of the jets in this event. The embedded pythia di-jet clearly is separated from the background jets.

Jet Performance

Performance for jet reconstruction is evaluated by embedding full PYTHIA di-jet events into unquenched HIJING events. The reconstructed jets are compared to truth jets that result from the same algorithms run on the PYTHIA final state particles. Fig. 3 shows the comparison of the cone and the k_T algorithm performance for dN/dη =2700 (b = 2 fm) HIJING backgrounds. It also shows the position (Δφ) resolutions as a function of E_T for different HIJING multiplicities. Finally the energy resolution for several HIJING event multiplicities is shown for the η full range of the ATLAS calorimeter.

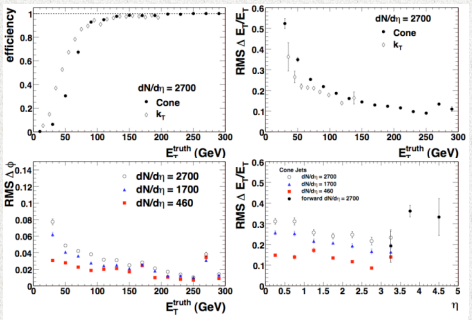

Fig. 3 *Upper:* Comparison of jet reconstruction efficiency (left) and jet energy resolution (right) of cone (filled circles) and k_T (open circles) reconstructed jets in unquenched HIJING with dN/dη= 2700. *Lower:* E_T-dependence of the position (Δφ) resolution (left) and η-dependence of the energy resolution (right) for cone jets for different HIJING multiplicities.

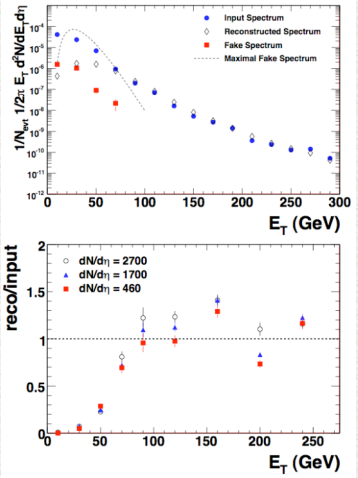

Fig. 4 *Upper:* Comparison of expected (blue circles), raw reconstructed (diamonds), and irreducible fake jet rate (red squares) for dN/dη =2700 Pb+Pb events. *Lower:* The ratio of the raw reconstructed to expected jet spectra for different HIJING event multiplicities. Before efficiency and energy resolution corrections the ratio is only 20% high.

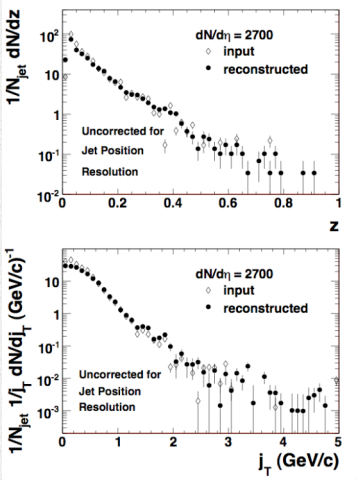

Fig. 5 Truth (diamonds) and reconstructed (filled circles) fragmentation function (upper) and j_T distribution (lower) built from charged tracks associated with jets. The reconstructed distributions are corrected for tracking efficiency but not for jet reconstruction energy or position resolutions.

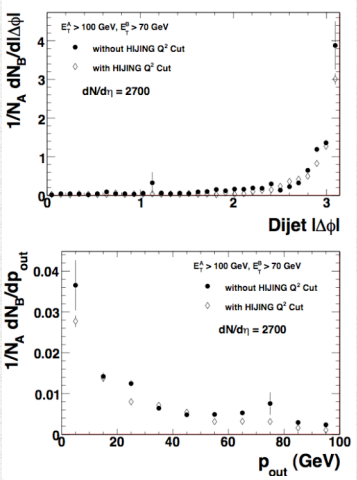

Fig. 6 Di-jet distributions in Δφ (upper) and p_{out} (lower). Distributions are not corrected for jet energy or position resolution or efficiency. The open points show the same distribution of di-jets in HIJING events where jets > 10 GeV have been removed.

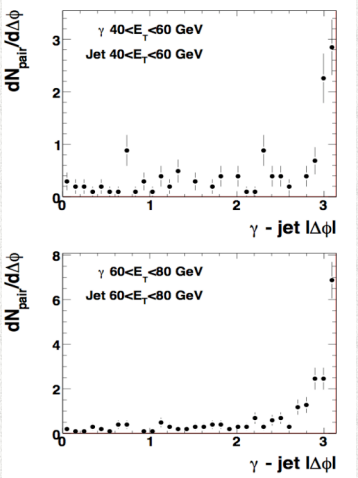

Fig. 7 Correlation between reconstructed photons and jets from HIJING events with PYTHIA γ-jet events embedded. Two different energy cuts are shown in the upper and lower panels.

Jet Energy Loss

Figures 4-7 outline the possible avenues of studying jet energy loss using fully reconstructed jets. First, Fig. 4 shows the expected jet rate based on binary scaled PYTHIA events for dN/dη=2700 (b=2 fm) HIJING events compared to the raw (uncorrected) reconstructed jet rate and the irreducible fake jet rate. Fake jets are removed post reconstruction by shape analysis. The ratio of reconstructed to expected jets is shown in the lower panel of Fig. 4 showing that at high-E_T the difference is only 20% before corrections. The rate of jets will be sensitive to radiation outside of the cone and elastic scattering in the medium. Fig. 5 shows the fragmentation function, D(z), and the j_T distribution of particles associated with truth jets and reconstructed charged tracks associated with reconstructed jets. The distributions are expected to be modified by jet energy loss as high-z fragments are shifted to lower z and hard radiation will populate the high-j_T tail of that distribution. Fig. 5 shows that the input distributions are well reproduced before corrections and sensitivity to their modification should be possible. Fig. 6 shows di-jet Δφ and p_{out} (= $E_T^B \sin\Delta\phi$) distributions using reconstructed jets. These distributions will be sensitive to multiple scattering of jets in the medium. Fig. 7 shows the correlation in Δφ of reconstructed γ and jets from embedded PYTHIA γ-jet events in unquenched HIJING. Using the γ directly will yield the fragmentation function of the recoil jet.

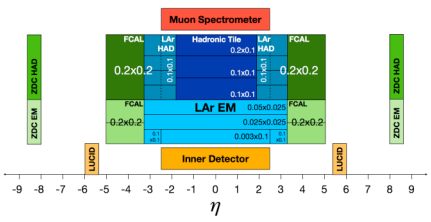

Fig. 8 Phase space coverage of the ATLAS detector. All detectors shown have full azimuthal coverage.